

than those in  $\text{XeF}_6$  and  $\text{ClF}_6^-$ , resulting in minimal concentration of charge on the *central* atom along the bond paths, i.e., very small, if any, bonded maxima for the nonbonded maximum to repel. In ref 6 the effects of electronegativity difference on the size of the bonded charge concentrations were reported. The effects were found to parallel the VSEPR argument that the bonded pair is more concentrated on the more electronegative atom; i.e., going from  $\text{NH}_3$  to  $\text{NF}_3$  the size of the bonded charge concentration on nitrogen *decreased*. Hence one would expect the bonded charge concentrations on tellurium in  $\text{TeCl}_6^{2-}$  to be much smaller than the corresponding ones in  $\text{XeF}_6$ , for example. In addition to a reduction in the size of the bonded charge concentrations on the central atom, the increase in electronegativity difference would also result in a more closed-shell-like interaction. As this work suggests, such an increase in the closed-shell nature of the atomic interactions would lead to increased fluxionality. These predictions could be tested by an analysis of the calculated charge distributions of  $\text{XeF}_6$  and  $\text{TeCl}_6^{2-}$ . Nevertheless this work suggests that any  $\text{AX}_6\text{E}$  system will show some, possibly very small, distortion from  $O_h$  symmetry in the gas phase arising from the presence of a nonbonded charge concentration on A.

Gimarc et al. have presented a qualitative MO argument to rationalize the observed symmetries of various  $\text{AX}_6\text{E}$  systems.<sup>26</sup> They argue that the larger the electronegativity difference between the central atom and the ligands, the less the distorted geometry will be stabilized by in-phase overlap of the ligand AO's comprising the totally symmetric HOMO. While this model makes the same predictions as above, it focuses on a single orbital. The atomic charges presented here suggest that the dominant ligand-ligand interaction (indirect since the fluorine atoms do not share an interatomic surface) is electrostatic repulsion, even when the electronegativity difference is minimized.

#### Connection between the SOJT Model and the Properties of the Charge Density

The SOJT model only requires knowledge of the symmetries of the lowest lying excited state (or unoccupied orbital) to make

predictions of chemical interest. The energies of the virtual orbitals are largely determined by the distribution of charge in the occupied orbitals. Thus the SOJT model is inherently dependent on the ground-state charge distribution. In the previous section, although it was clear from just the properties of the charge distribution that  $\text{ClF}_6^-$  would be a very fluxional molecule, it was not clear *how* the molecule would most easily undergo this fluctuation. The SOJT model was used to determine the symmetry of this process. Perhaps information contained in the Laplacian distribution may provide a link between the static properties described by  $\rho_{00}$ , which can be determined experimentally, and the dynamical properties described by  $\rho_{0k}$ , which cannot. For instance in  $\text{ClF}_6^-$  there are three possible transition states that would lead to pseudorotation:  $C_{2v}$ ,  $C_{4v}$ , and  $O_h$ . Along the lines of the VSEPR model the  $C_{2v}$  transition state minimizes the repulsive interactions between bonded and nonbonded charge concentrations that are less than  $90^\circ$  apart; hence, the easiest pathway for pseudorotation should be through a  $C_{2v}$  transition state, as is found.

**Acknowledgment.** I thank the Xerox Research Centre of Canada for the award of a Graduate Research Fellowship during 1984-1985.

**Note Added in Proof.** Within the framework of the present theory<sup>14</sup> one can partition the fluxional activation barrier into atomic contributions,  $\Delta E(\Omega) = E(\Omega)_{\text{trans}} - E(\Omega)_{\text{equil}}$ .  $\Delta E(\Omega) > 0$  indicates the atom is less stable in the transition state, while  $\Delta E(\Omega) < 0$  indicates the opposite. A similar partitioning of singlet-triplet energy gaps in carbenes has recently been reported.<sup>18</sup> With respect to the numbering scheme in Figure 4, the values for  $\text{ClF}_6^-$  are as follows (kcal/mol):  $\Delta E(\text{Cl}) = -17$ ,  $\Delta E(\text{F1}) = +44$ ,  $\Delta E(\text{F2(3)}) = -8$ ,  $\Delta E(\text{F4}) = -7$ ,  $\Delta E(\text{F5(6)}) = -1$ . The corresponding values for  $\text{ClF}_3$  are as follows (kcal/mol):  $\Delta E(\text{Cl}) = -26$ ,  $\Delta E(\text{F}_{\text{ax}}) = +57$ ,  $\Delta E(\text{F}_{\text{eq}}) = -42$ . These numbers are to be compared with the data in Table II. Interestingly, the chlorine atom becomes *more* stable in the transition state for both systems. As should be expected, the destabilization in both systems is incurred by removing electrons from one or more fluorine atoms. It is instructive that it costs more energy to remove 0.03 e from the axial fluorine in  $\text{ClF}_3$  (initially  $q = -0.52$  e) than to remove 0.16 e from F1 in  $\text{ClF}_6^-$  (initially  $q = -0.66$  e). While there are additional factors determining  $\Delta E(\Omega)$ , we feel that these data suggest that the fluxional behavior of these, and presumably other similar systems, strongly depends on the extent of "saturation" of the ligands.

**Registry No.**  $\text{ClF}_6^-$ , 42278-52-4.

(26) Gimarc, B. M.; Liebman, J. F.; Kohn, M. J. *Am. Chem. Soc.* **1978**, *100*, 2334.

Contribution from the Chemistry Department, University of British Columbia, Vancouver, BC, Canada V6T 1Y6

## Mass Spectral Studies on the Thermal Decomposition of $\text{S}_4\text{N}_4$ and the Mechanism for Formation of $(\text{SN})_x$

Elizabeth Besenyei,<sup>†</sup> Guenter K. Eigendorf, and David C. Frost\*

Received March 25, 1986

A mechanism for the polymerization of  $(\text{SN})_x$  is proposed on the basis of a mass spectrometric study of the thermal decomposition of  $\text{S}_4\text{N}_4$ . The temperature dependence of the relative ion abundances and also the appearance potentials of the spectral fragments originating from  $\text{S}_4\text{N}_4$  and  $\text{S}_2\text{N}_2$  indicate that thermal decomposition produces these fragments as neutral species. We propose a fragmentation scheme in which reactions in the main pathway from  $\text{S}_4\text{N}_4$  to  $\text{SN}$  are reversible and side reactions leading to loss of nitrogen and sulfur are not. In the presence of silver wool the transformation of  $\text{S}_2\text{N}_2$  to  $(\text{SN})_2$  occurs, the latter being the starting material for the polymer. Both the thermal fragmentation of  $\text{S}_4\text{N}_4$  to  $\text{S}_2\text{N}_2$  and the transformation of  $\text{S}_2\text{N}_2$  to  $(\text{SN})_2$  are facilitated by increasing the temperature, which also leads to the loss of nitrogen atoms. The polymerization process involves the reaction of  $(\text{SN})_2$  with  $\text{SN}$  originating from  $\text{S}_2\text{N}_2$ .

### Introduction

Tetrasulfur tetranitride ( $\text{S}_4\text{N}_4$ ) is the most well-known and characterized sulfur-nitrogen compound and provides the starting material for much chemistry in this area (see the reviews by Heal<sup>1,2</sup> and Labes et al.<sup>3</sup>).

Among the many diverse reactions of  $\text{S}_4\text{N}_4$ , thermal decomposition is of particular interest, since it leads to the synthesis of the unusual anisotropic three-dimensional metallic polymer  $(\text{SN})_x$ .

- (1) Heal, H. G. *Adv. Inorg. Chem. Radiochem.* **1972**, *15*, 375.
- (2) Heal, H. G. *The Inorganic Heterocyclic Chemistry of Sulfur, Nitrogen and Phosphorus*; Academic: London, 1980; p 115.
- (3) Labes, M. M.; Love, P.; Nichols, F. L. *Chem. Rev.* **1979**, *79*, 1.
- (4) Mikulski, C. M.; Russo, P. J.; Saran, M. S.; MacDiarmid, A. G.; Garito, A. F.; Heeger, A. J. *J. Am. Chem. Soc.* **1975**, *97*, 6358.
- (5) Cohen, M. J.; Garito, A. F.; Heeger, A. J.; MacDiarmid, A. G.; Mikulski, C. M.; Saran, M. S.; Kleppinger, J. *J. Am. Chem. Soc.* **1976**, *98*, 3844.

\* To whom correspondence should be addressed.

<sup>†</sup> Permanent address: Microelectronic Enterprise, 1044-Budapest, Hungary, F6ti U. 56.

Disulfur dinitride  $S_2N_2$  is the major product obtained by passing  $S_4N_4$  over silver, Pyrex, or quartz wool at 200–300 °C. The  $S_2N_2$  vapor condenses as a colorless diamagnetic solid that rapidly becomes blue and paramagnetic when warmed. It then slowly polymerizes to form diamagnetic  $(SN)_x$ . The identities and relative abundances of other products and intermediates involved in these reactions as well as the sulfur nitride radical SN have been detected ( $S_2N_2$ ,  $S_3N_3$ , and SN are said to occur in this system as main products<sup>6–9</sup>). An acyclic isomer of  $S_4N_4$ ,  $(SN)_4$ , previously thought to be the major sublimation product of  $(SN)_x$ , has been suggested as the "primary intermediate".<sup>7,10</sup> A mass spectrometric study<sup>9</sup> showed the direct pyrolysis products from  $S_4N_4$  to be a mixture including  $S_4N_4$ ,  $S_3N_3$ ,  $S_2N_2$ ,  $S_3N$ ,  $S_2N$ , and  $S_2$ . More recently,<sup>11</sup> the hitherto unknown  $S_3N_3$  radical has been found to be the major product of vaporization of the  $(SN)_x$  polymer. However, the precursor(s) to  $(SN)_x$ , as well as the process of polymerization still remain unknown.

$S_2N_2$ , besides being an intermediate in the formation of  $(SN)_x$ , is an interesting species on its own account. Its molecular geometry has been shown by X-ray crystallography<sup>12</sup> to be square planar with alternating S and N atoms, with bond lengths almost equal (average value 1.654 Å). The chemical and physical properties have been extensively reviewed.<sup>1–3</sup> The colorless crystals polymerize to  $(SN)_x$  even at 0 °C and can be sublimed at  $10^{-2}$  torr.

The electronic structure of  $S_2N_2$  has been studied by He I<sup>13,14</sup> and He II<sup>15</sup> photoelectron spectroscopy, and several theoretical calculations,<sup>15–19</sup> including an investigation of the mechanism of polymerization, have been made.

In the preparation of colorless  $S_2N_2$  from  $S_4N_4$ , several authors have noted the presence of various colored species, described at times as pink, red, and orange side products. Several of these have been isolated and some found to polymerize to form golden lustrous crystals of  $(SN)_x$ .<sup>20</sup> Another is a dark red, crystalline paramagnetic species, solid at room temperature, which appears to be the SN radical, and yet another, a dark brown, crystalline monomer with a molecular weight of 92. This last species was not identified; however, we refer to it as  $(SN)_2$ , using now, as throughout this paper, the convention that units of  $(SN)_x$  for various values of  $x$  refer to units of the polymer. The SN radical is different from yet another side product, the well-known  $S_4N_4$ ,<sup>21</sup> which has been shown<sup>4</sup> to appear as an impurity in  $(SN)_x$ .

Love et al.<sup>20</sup> report that polymerization of SN,  $S_2N_2$ , and  $(SN)_2$  takes hours, days, and minutes, respectively, and also that the polymers arising from the first two appear to be identical.

We report here a study of the thermal decomposition of  $S_4N_4$  at different temperatures with and without silver wool present, from which we are able to propose a polymerization mechanism that is consistent with some earlier unexplained observations. We rely to a large extent on mass spectral appearance potentials (AP's) and ionic relative abundances.

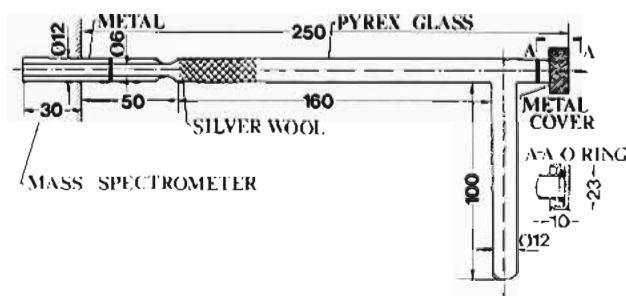


Figure 1. Probe II (dimensions in mm).

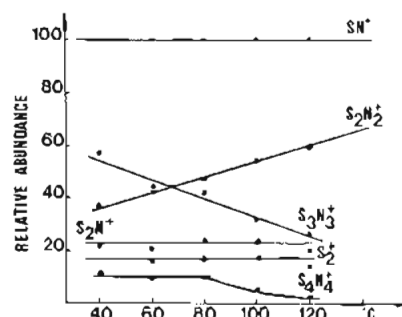


Figure 2. Mass spectral data arising from  $S_4N_4$  pyrolysis (indirect probe I).

Table I. Relative Abundances of Principal Ions in Mass Spectra of  $S_4N_4$ <sup>a</sup>

ion	m/z	temp of sample tube, °C					direct probe III 80
		indirect probe I					
		40	60	80	100	120	
$SN^+$	46	100	100	100	100	100	100
$S_2^+$	64	22	16	17	17	14	11
$S_2N^+$	78	22	21	24	23	20	21
$S_2N_2^+$	92	37	42	47	54	59	62
$S_3N^+$	110		2	4	4	4	4
$S_3N_2^+$	124		1	6	3	1	3
$S_3N_3^+$	138	57	44	42	32	26	82
$S_4N_2^+$	156		0.5	6	4	5	
$S_4N_4^+$	184	11	10	10	5	2	16

<sup>a</sup>All abundances represent the average of nine or more measurements. Reproducibility is  $\pm 20\%$  of the value.

## Experimental Section

$S_4N_4$  was prepared from  $S_2Cl_2$  and ammonia,<sup>22</sup> purified by recrystallization from toluene, and sublimed in vacuo before use. Infrared spectra<sup>22</sup> (KBr pellet), melting point (found 184.5–186 °C, literature value 178–187 °C),<sup>24</sup> and microanalytical data revealed no impurities of consequence. The silver wool was cleaned by heating.<sup>25</sup>

Mass spectra were recorded on a Vacuum Generators Micromass-12 mass spectrometer under the following conditions unless otherwise noted: 150 °C ion source temperature, 4-kV acceleration voltage, and 70-eV electron energy. Samples were introduced into the ion source via an indirect probe (probe I), which allowed independent heating of the sample and source and control of the vapor pressure in the spectrometer. The sample was placed in a glass tube heated by an oil bath (the primary sample region). Electrical heating tape was used to heat the remainder of the probe, a stainless-steel tube of diameter 6 mm and length 56 cm.

The temperature of the tube above the sample was monitored by three thermometers and could be held to  $\pm 10$  °C. The sample temperature could be maintained to  $\pm 2$  °C.  $S_2N_2$  was prepared by vaporizing  $S_4N_4$  (50–60 °C) and passing it over heated silver wool.<sup>4</sup>  $S_2N_2$  vapor entered the mass spectrometer source through an orifice located  $\sim 5$  cm beyond 3.3 g of the wool (see Figure 1, which shows a second probe, II), occupying 40 mm of a 0.12 mm diameter (o.d.) Pyrex tube. Probe II was

- Smith, R. D.; Wyatt, J. R.; Decorpo, J. J.; Saalfeld, F. E. *Chem. Phys. Lett.* **1976**, *41*, 362.
- Smith, R. D.; Wyatt, J. R.; Decorpo, J. J.; Saalfeld, F. E.; Moran, M. J.; MacDiarmid, A. G. *J. Am. Chem. Soc.* **1977**, *99*, 1726.
- Smith, R. D. *Chem. Phys. Lett.* **1978**, *55*, 590.
- Smith, R. D. *J. Chem. Soc., Dalton Trans.* **1979**, 478.
- Caranagh, R. R.; Altman, R. S.; Herschbach, D. R.; Klemperer, W. J. *Am. Chem. Soc.* **1979**, *101*, 4734.
- Lau, W. M.; Westwood, P.; Palmer, M. H. *J. Chem. Soc., Chem. Commun.* **1985**, 752.
- MacDiarmid, A. G.; Mikulski, C. M.; Russo, P. J.; Saran, M. S.; Garito, A. F.; Heeger, A. J. *J. Chem. Soc., Chem. Commun.* **1975**, 476.
- Findlay, R. H.; Palmer, M. H.; Dawas, A. J.; Egdell, R. G.; Evans, R. *Inorg. Chem.* **1980**, *19*, 1307.
- Frost, D. C.; LeGeyt, M. R.; Paddock, N. L.; Westwood, N. P. C. *J. Chem. Soc., Chem. Commun.* **1977**, 217.
- Salahub, D. R.; Messner, R. P. *Phys. Rev. A* **1976**, *14*, 2592.
- Yamabe, T.; Tanaka, K.; Fukui, K.; Kato, H. *J. Phys. Chem.* **1977**, *81*, 727.
- Palmer, M. H.; Findlay, R. H. *J. Mol. Struct.* **1983**, *92*, 373.
- Tang, T.; Bader, R. F. W.; MacDougall, P. J. *Inorg. Chem.* **1985**, *24*, 2047.
- Haddon, R. C.; Wasserman, S. R.; Wudl, F.; Williams, G. R. *J. Am. Chem. Soc.* **1980**, *102*, 6687.
- Miller, J. S.; Epstein, A. J. *Ann. N. Y. Acad. Sci.* **1978**, *313*, 745.
- Nelson, J.; Heal, H. G. *J. Chem. Soc. A* **1971**, 136.

- Arnold, M. H.; Hugill, J. A. C.; Hutson, J. M. *J. Chem. Soc.* **1936**, 1645.
- Bragin, J.; Evans, M. V. *J. Chem. Phys.* **1969**, *51*, 268.
- Villena-Blanco, M.; Jolly, W. L. *Inorg. Synth.* **1967**, *9*, 98.
- Ingram, G. *Methods of Organic Elemental Analysis*; Hall: London, **1962**; p 62.

**Table II.** Appearance Potentials of Mass Spectral Fragments from  $S_2N_2$  (Condition 3) and  $S_4N_4$  (Conditions 1 and 2)

ion	$m/z$	appearance potentials, eV			known ionizn potential, eV	ref
		1 no silver wool sample (60 °C)	2 silver wool (100 °C) sample (60 °C)	3 silver wool (220 °C) sample (45 °C)		
$SN^+$	46	9.1	9.1	9.3	8.87	29
$S_2^+$	64	9.7	9.7	9.7	9.7	30
$S_2N^+$	78	9.7				
$S_2N_2^+$	92	10.2	10.3	10.3	10.52	14
$S_3N^+$	110	9.9				
$S_3N_2^+$	124	8.7				
$S_3N_3^+$	138	8.8	8.6		8.62	11
$S_4N_2^+$ <sup>a</sup>	156	9.2				
$S_4N_4^+$	184	9.5	9.3		9.36	12

<sup>a</sup> $S_4N_2^+$  measured at 100 °C in probe I.

heated in the same way as probe I. For reasons given later, a direct probe (probe III) was used to evaporate  $S_4N_4$  into a mass spectrometer having a lower inlet temperature, a KRATOS MS50 with 70-eV electron energy, 80 °C inlet temperature, 8-kV acceleration voltage, and resolution of  $m/z \sim 1000$ .

All the reported measurements were made after allowing at least 30 min to reach a steady state at each temperature. Pressures in the ion source were dependent on the temperature of the  $S_4N_4$  sample.

Twenty-five determinations were made for each appearance potential (AP) by using the extrapolated voltage difference technique,<sup>26</sup> with argon and methyl iodide as calibrant gases. We recorded relative abundances of ions of  $m/z > 40$  only.

### Results and Discussion

The temperature dependence of the mass spectra of  $S_4N_4$  pyrolysis products, determined by using indirect probe I and direct probe III, is shown in Table I. The stainless-steel tube was held at 100 °C to prevent condensation in that region.

The major ions resulting from the pyrolysis of  $S_4N_4$  are  $S_3N_3^+$ ,  $S_2N_2^+$ ,  $S_3N^+$ ,  $S_2^+$ , and  $SN^+$ , with relatively smaller abundances of  $S_4N_4^+$ ,  $S_4N_2^+$ ,  $S_3N_2^+$ , and  $S_3N^+$ . Clearly, from Table I, the heavier fragment ions become relatively less abundant at higher temperatures. Above 80 °C  $S_2N_2^+$  becomes the second largest peak (probe I) and the ratio of  $S_3N_3^+/S_2N_2^+ < 1$ . Data obtained with probe III indicate that reversal to be due to the higher vapor temperature, the sample itself remaining at 80 °C. When probe I was used, the temperature of the rather long metal tube  $T_2$  was held at 100 °C and the source temperature at 150 °C, and so the actual temperature of the vapor was certainly  $> 80$  °C.  $S_3N^+$ ,  $S_3N_2^+$ , and  $S_4N_2^+$  all appear as the  $S_4N_4$  temperature is increased; the relative abundance of  $S_4N_4^+$  decreases, while the total vapor pressure in the ion source increases due to the higher sample temperature. Smith<sup>8</sup> found that heating  $S_4N_4$  led to  $S_3N_3^+$  as the base peak, unlike Butler et al.,<sup>27</sup> who found it to be  $SN^+$ . The electron energy used by Smith was 16 eV and by Butler et al. 70 eV. In an attempt to clarify this situation, we measured the mass spectra dependence on electron energy (Figure 3). The temperature of the sample was 100 °C (probe I).

Quite clearly, the mass spectrum is very energy-dependent and explains the discrepancies between the previous data mentioned.<sup>8,27</sup>

In order to investigate the polymerization mechanism of  $S_2N_2$ , we placed some  $S_4N_4$  in probe II, put silver wool in the upper part of the tube (Figure 1), and recorded the mass spectra of the products formed at several wool temperatures. The results are given in Figure 4.

The temperature of the sample reservoir was maintained below 60 °C to prevent excessive gas pressure in the spectrometer, and as the temperature of the silver wool ( $T_{Ag}$ ) was increased to 200 °C, so the sample temperature was decreased to maintain a spectrometer pressure of  $< 10^{-5}$  torr. Indications are that the vapor pressure of  $S_2N_2$  exceeds that of the other species, and so as the quantity of  $S_2N_2$  increases, so does the pressure in the system. With  $T_{Ag}$  at 220 °C, we observe on the sample tube wall (at 60 °C) a blue-black film that becomes thicker as  $T_{Ag}$  increases. At

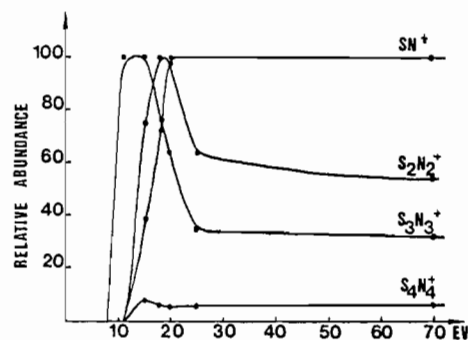


**Figure 3.** Principal mass spectral peaks from  $S_4N_4$  at 100 °C (sample) from 8- to 70-eV electron energy.

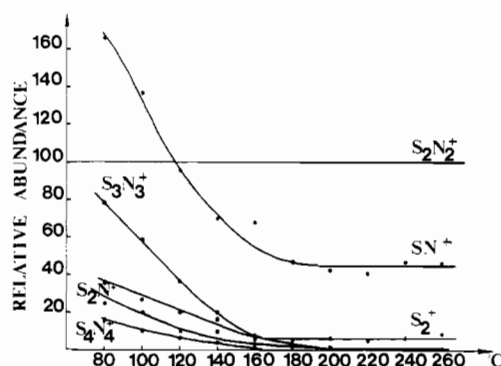


**Figure 4.** Relative abundances of some mass spectral fragments from  $S_4N_4$  at various silver wool temperatures.

the same time, the mass spectra gradually change: above 120 °C  $S_2N_2^+$  becomes the main peak,  $S_4N_4^+$  and  $S_3N_3^+$  gradually decrease, and above 180 °C peaks higher than  $m/z$  92 are barely seen. We saw no  $S_4N_2^+$ , probably due to the low temperature of the sample, which points to  $S_4N_2^+$  originating directly from  $S_4N_4$  itself, not from its decomposition products. This agrees with the findings of Smith et al.<sup>8</sup> insofar as they found  $S_4N_2^+$  during the decomposition of  $S_4N_4$  over both quartz and silver wool, indicating that silver wool does not play a unique role in  $S_4N_2$  formation. Previous workers<sup>28</sup> have suggested a mechanism involving sulfur formation on silver wool surfaces with a subsequent reaction with  $S_2N_2$  to form  $S_4N_2$ . We feel this to be incorrect (vide infra).

The ratio  $S_2N_2^+/S_3N_3^+$  is  $> 1$  in the presence of silver wool (80–60 °C) with probe II. However, with no wool the ratio is  $< 1$ . This is an important observation regarding the role of the wool (see below). Both  $S_2N^+$  and  $S_2^+$  peaks decrease as  $T_{Ag}$  changes from 80 °C to 180 °C, above which the ratio of

(26) Warren, J. W.; McDowell, C. A. *Discuss. Faraday Soc.* **1951**, 10, 53.

(27) Butler, J. S.; Sawai, T. *Can. J. Chem.* **1977**, 55, 3838.

(28) Douillard, A.; Mag, J.; Vallet, G. *Ann. Chim. (Paris)* **1971**, 6, 257.

(29) Dyke, J. M.; Morris, A.; Frickle, J. R. *J. Chem. Soc., Faraday Trans. 2* **1977**, 73, 147.

(30) *Natl. Stand. Ref. Data Ser. (U.S., Natl. Bur. Stand.)* **1969**, NSRDS-NBS 26.

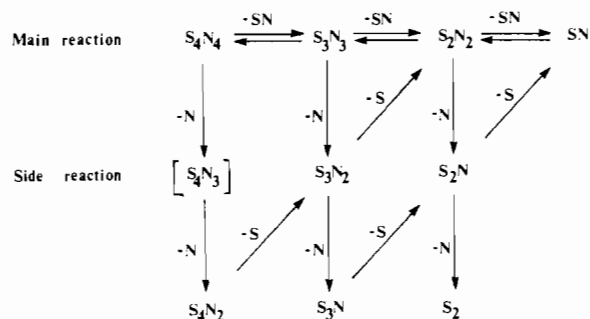


**Figure 5.** Fragmentation scheme for thermal decomposition of S<sub>4</sub>N<sub>4</sub> (the existence of S<sub>4</sub>N<sub>3</sub> is, we feel, a reasonable postulation).

S<sub>2</sub>N<sub>2</sub><sup>+</sup>/SN<sup>+</sup>/S<sub>2</sub><sup>+</sup>/S<sub>2</sub>N<sup>+</sup> remains almost constant.

In order to determine the decomposition mechanism and also if possible the bond energies in S<sub>4</sub>N<sub>4</sub>, we measured the appearance potentials (AP's) of some fragment ions formed from S<sub>2</sub>N<sub>4</sub> and S<sub>4</sub>N<sub>4</sub> (probe II). The results are shown in Table II.

AP's measured in the absence of silver wool showed little variation with sample temperature (60–100 °C). Our results (Table II) show that the AP's of the different fragments do not depend on the nature of the parent molecule, and hence these fragments must arise from thermal decomposition of molecular precursors and not (at their AP's) by dissociative ionization. We note that Smith et al.<sup>7</sup> report much higher AP's for many of the fragment ions, but significantly the ionization energy found for S<sub>2</sub>N<sub>2</sub> by them (11.5 eV) is 1 eV higher than the other literature value.<sup>14</sup>

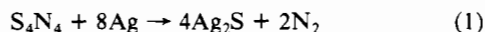
Thermal fragmentation begins at a sample reservoir temperature as low as 40 °C (the vapor temperature was higher), and only the ratios of the molecular concentrations change during vaporization (due to temperature differences); however, the main pathways of thermal fragmentation do not change. The molecular ratios depends on equilibria, and hence temperature, and we conclude this to be the main reason for the spectral changes.

The fragmentation scheme proposed originally by Butler and Sawai<sup>27</sup> seems to be acceptable, but the molecules shown in Figure 5 must be in equilibrium, their relative abundances dependent of course on temperature.

Our spectra lead us to conclude that as the temperature is varied, so are the concentrations of the molecular species S<sub>4</sub>N<sub>4</sub>, S<sub>3</sub>N<sub>3</sub>, S<sub>2</sub>N<sub>2</sub>, and SN; they coexist in the gas phase, and their relative vapor pressures are temperature-dependent. The "main reactions" are all reversible; however, the "side reactions" are not, and although the rates of all six will of course increase with temperature, each individual concentration remains linked to its parent's concentration in the "main reaction" system. This explanation provides a rationale for the vaporization process, but not for the polymerization.

The most plausible mechanism for polymerization that involves S<sub>2</sub>N<sub>2</sub> units utilizes the "principle of least motion".<sup>5</sup> Initial ring opening of an S<sub>2</sub>N<sub>2</sub> molecule followed by repetitive attack upon adjacent S<sub>2</sub>N<sub>2</sub> molecules down the crystal axes could yield the polymer. Experimental evidence involving "partially polymerized S<sub>2</sub>N<sub>2</sub>" crystallographic studies<sup>5</sup> suggests this as an acceptable approach. Deformation of S<sub>2</sub>N<sub>2</sub> to the monomeric (SN)<sub>2</sub> unit is endothermic by ca. 1–4 eV depending on the electronic state involved.<sup>17</sup> An alternative mode of polymerization—decomposition of S<sub>2</sub>N<sub>2</sub> to SN followed by serial attack on S<sub>2</sub>N<sub>2</sub> molecules<sup>31</sup> seems to be highly unlikely.<sup>17</sup>

The supposed role of silver wool<sup>3</sup> to produce S<sub>2</sub>N<sub>2</sub> molecules is



followed by Ag<sub>2</sub>S catalysis of thermal cleavage

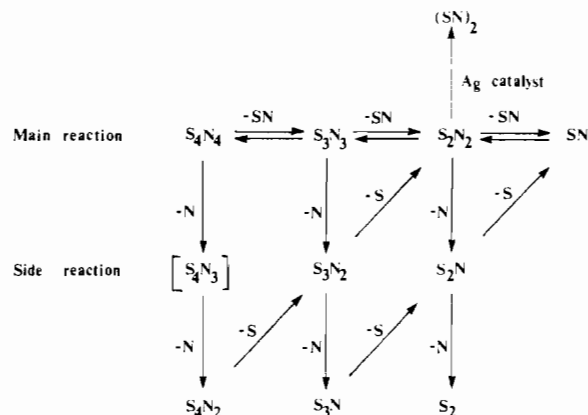
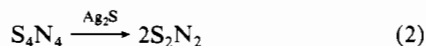


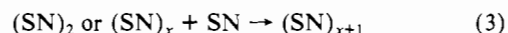
**Figure 6.** Complete fragmentation scheme for the thermal decomposition of S<sub>4</sub>N<sub>4</sub> in the presence of silver wool.

Considering the calculations mentioned above and our mass spectral studies on the decomposition process over silver wool, we propose that the processes outlined in Figure 5 must be completed by another concurrent reaction, namely the transformation of S<sub>2</sub>N<sub>2</sub> to (SN)<sub>2</sub>, as shown in Figure 6.

Calculations<sup>17</sup> indicate the ionization energy difference between S<sub>2</sub>N<sub>2</sub> and (SN)<sub>2</sub> to be within our experimental error (±0.3 eV). The mechanism we propose explains the change in relative abundances of S<sub>2</sub><sup>+</sup> and S<sub>2</sub>N<sup>+</sup> (seen in Figure 4) since their source (S<sub>2</sub>N<sub>2</sub>) decreases. Silver wool probably plays an important role in the transformation of S<sub>2</sub>N<sub>2</sub> to (SN)<sub>2</sub>, catalyzing this endothermic reaction. Probably the yield of (SN)<sub>2</sub> will increase with the temperature of the decomposition zone containing either silver wool or quartz wool, but in the absence of silver the loss of N becomes predominant and leads to the total decomposition of S<sub>4</sub>N<sub>4</sub> (which agrees with the findings of ref 8).

The amount of quartz or silver wool affects the time to reach the "quasi-equilibrium" concentration at a given temperature, which would explain the reaction dependence on the amount of wool observed by Smith et al.<sup>8</sup> The pressure of the system plays a similar role.

We propose the starting material for the polymerization to be (SN)<sub>2</sub> and the polymerization process to involve (SN)<sub>2</sub> reacting with SN:



The SN radical is generated from S<sub>2</sub>N<sub>2</sub> as the last main reaction step of Figure 6. This mechanism is in accord with observations on the different polymerization rates of various monomers.<sup>20</sup> The brown monomer, mainly (SN)<sub>2</sub>, has the fastest polymerization rate (within minutes), the red (SN radicals) has the second fastest polymerization rate (within hours), and the colorless S<sub>2</sub>N<sub>2</sub> polymerizes over a period of days. Probably (SN)<sub>2</sub> is present in every case, but in different amounts. The polymerization of (SN)<sub>2</sub> must be rapid since units need only bond adjacently—no other reaction need be invoked. The reaction between (SN)<sub>2</sub> and SN or (SN)<sub>x</sub> and SN should be slower, by similar reasoning. In the third case the slowest step is the reaction to produce SN radicals for the polymerization, which could be very slow in the solid state.

We can also comment on the three crystal structures reported in (SN)<sub>x</sub>.<sup>20</sup> The structures of the polymers arising from the red SN monomer and the colorless S<sub>2</sub>N<sub>2</sub> structure should be very similar, since they form in exactly the same way. In the third, the "open" (SN)<sub>2</sub>, the bond lengths, which will be similar to those in S<sub>2</sub>N<sub>2</sub>, should be closely followed in the polymer, there being insufficient time for significant change during the polymerization process. The consequent stress in this (SN)<sub>x</sub> explains its instability (2 days or less).

(SN)<sub>x</sub> sublimation was another aspect examined in an attempt to determine the nature of the precursor(s).<sup>6,7,11</sup> Our theory predicts the molecules to be linear (the highest number of atoms dependent on the stability of the structure, namely S<sub>3</sub>N<sub>3</sub> or S<sub>4</sub>N<sub>4</sub>) because there is no sign of distortion of the polymer during sublimation and the repolymerization process is very fast. If the

(31) Baughman, R.; Chance, R. R.; Cohen, M. J. *J. Chem. Phys.* **1976**, *64*, 1869.

same steps have to be repeated, the process will be slower or distortion will result. Examining the sublimation of  $(\text{SN})_x$ , by photoionization mass spectrometry, Lau et al.<sup>11</sup> found only  $\text{S}_3\text{N}_3$ , and no  $\text{S}_2\text{N}_2$  or  $\text{SN}$ , probably due to the low photon energy (10.2 eV) used (see our Figure 3—the energy dependence of the mass spectrum).

The polymerization process itself appears to have two important steps; the first is the fragmentation to  $\text{S}_2\text{N}_2$ , and the second is the transformation of  $\text{S}_2\text{N}_2$  to  $(\text{SN})_2$ . Both are facilitated by using higher temperatures or catalysts. At the same time, increasing the temperature may lead to side reactions involving loss of N. The quantity of  $(\text{SN})_2$  is critical; if there is "too much" during the reaction, the polymer quality will be degraded. From Figure 6 it is clear that the best way to obtain the polymer is to use a small amount of  $(\text{SN})_2$  and to move the  $\text{S}_2\text{N}_2 \rightarrow \text{SN}$  equilibrium in favor of  $\text{SN}$ .

### Conclusions

On the basis of thermal decomposition of  $\text{S}_4\text{N}_4$  over and in the absence of silver wool, as well as considering appearance potentials

of different mass spectral fragments originating from  $\text{S}_4\text{N}_4$  and  $\text{S}_2\text{N}_2$ , we propose a mechanism for the  $(\text{SN})_x$  polymerization process. This mechanism explains some conflicting observations reported by previous workers and includes two important steps—the fragmentation of  $\text{S}_4\text{N}_4$  to  $\text{S}_2\text{N}_2$  and the transformation of  $\text{S}_2\text{N}_2$  to  $(\text{SN})_2$ . Both steps are facilitated by increasing the temperature, which also results in nitrogen atom loss. In the first step the large surface of different wools brings quick quasi-equilibrium; the second is affected by temperature and/or the presence of silver wool as a catalyst. The polymerization process involves the reaction of  $(\text{SN})_2$  with  $\text{SN}$  originating from  $\text{S}_2\text{N}_2$ .

**Acknowledgment.** This work was supported by grants from the NSERC of Canada. We are grateful to Professor N. L. Paddock for the starting material  $\text{S}_4\text{N}_4$  and for many stimulating discussions.

**Registry No.**  $\text{S}_4\text{N}_4$ , 28950-34-7; Ag, 7440-22-4;  $\text{S}_2\text{N}_2$ , 25474-92-4;  $(\text{SN})_x$ , 56422-03-8.

Contribution from the Department of Chemistry,  
Florida Atlantic University, Boca Raton, Florida 33431

## Electrochemical Reduction of Seven-Coordinate Oxomolybdenum(VI) Complexes. Multielectron Transfer at Mononuclear $\text{MoO}^{4+}$ Centers

Julie R. Bradbury<sup>1</sup> and Franklin A. Schultz\*

Received May 22, 1986

The seven-coordinate oxomolybdenum(VI) complexes  $\text{MoOX}_2(\text{S}_2\text{CNET}_2)_2^{n+}$  ( $\text{X}_2 = 2\text{Cl}^-$ ,  $2\text{Br}^-$ , catechol (cat) ( $n = 0$ );  $\text{X}_2 = \text{Et}_2\text{NCS}_2^-$  ( $n = 1$ )) undergo two-electron electrochemical reduction in nonaqueous solvents. Changes in Mo coordination number accompany electron transfer and provide the driving force for multielectron behavior. Evidence suggests that one metal–ligand bond is broken in conjunction with each electron addition and that the pathway of electrochemical reduction is seven-coordinate  $\text{Mo(VI)} \rightarrow$  six-coordinate  $\text{Mo(V)} \rightarrow$  five-coordinate  $\text{Mo(IV)}$ . Depending on the identity of  $\text{X}_2$ , this two-electron change appears as either a single two-electron transfer or two closely spaced one-electron transfers.  $\text{MoOCl}_2(\text{S}_2\text{CNET}_2)_2$  is reduced to  $\text{MoO}(\text{S}_2\text{CNET}_2)_2 + 2\text{Cl}^-$  in a two-electron step.  $\text{MoO}(\text{S}_2\text{CNET}_2)_2$  is reoxidized to  $\text{MoOCl}_2(\text{S}_2\text{CNET}_2)_2$  in the presence of  $\text{Cl}^-$ , but at a potential  $\sim 1$  V more positive than  $\text{Mo(VI)}$  reduction. Thus, the two-electron interconversion of  $\text{MoOCl}_2(\text{S}_2\text{CNET}_2)_2$  and  $\text{MoO}(\text{S}_2\text{CNET}_2)_2 + 2\text{Cl}^-$  is highly irreversible.  $\text{MoO}(\text{S}_2\text{CNET}_2)_3^+$  and  $\text{MoO}(\text{cat})(\text{S}_2\text{CNET}_2)_2$  complexes with electron-withdrawing catechol substituents ( $\text{Cl}_4\text{cat}$ ,  $\text{NO}_2\text{cat}$ ) exhibit  $\text{Mo(VI)/Mo(V)}$  and  $\text{Mo(V)/Mo(IV)}$  reduction waves separated by  $\sim 0.2$  V.  $\text{Mo(VI)/Mo(V)}$  reduction is chemically reversible for these tris(bidentate) species because cleavage of one metal–ligand bond does not displace a bidentate ligand from the molecule and the bond is easily re-formed upon reoxidation to  $\text{Mo(VI)}$ .  $\text{MoO}(\text{cat})(\text{S}_2\text{CNET}_2)_2$  complexes with electron-donating substituents (cat, DTBcat) also exhibit separate  $\text{Mo(VI)/Mo(V)}$  and  $\text{Mo(V)/Mo(IV)}$  reduction waves, but a rapid chemical reaction following the first charge transfer causes more than one electron to be transferred at the potential of  $\text{Mo(VI)}$  reduction.

### Introduction

The oxomolybdenum(VI) center ( $\text{MoO}^{4+}$ ), which typically exhibits seven-coordinate pentagonal-bipyramid geometry,<sup>2</sup> is becoming an increasingly common structural feature in molybdenum chemistry.<sup>3–11</sup> In contrast to more numerous *cis*-dioxo

$\text{MoO}_2^{2+}$  complexes, whose redox properties have been widely studied,<sup>12</sup> relatively few electrochemical investigations have been

- (1) Current address: Department of Chemistry, Washington University, St. Louis, MO 63130.
- (2) (a) Drew, M. G. *Prog. Inorg. Chem.* **1977**, *23*, 67. (b) Melnik, P.; Sharrock, P. *Coord. Chem. Rev.* **1985**, *65*, 49.
- (3) (a) Stiefel, E. I. *Prog. Inorg. Chem.* **1977**, *22*, 1. (b) Stiefel, E. I. In *Molybdenum and Molybdenum-Containing Enzymes*; Coughlan, M. P., Ed.; Pergamon: Oxford, England, 1980; Chapter 2.
- (4) Dirand, J.; Ricard, L.; Weiss, R. *J. Chem. Soc., Dalton Trans.* **1976**, 278.
- (5) Dirand, J.; Ricard, L.; Weiss, R. *Transition Met. Chem. (Weinheim, Ger.)* **1975**, *1*, 2.
- (6) Liebeskind, L. S.; Sharpless, K. B.; Wilson, R. D.; Ibers, J. A. *J. Am. Chem. Soc.* **1978**, *100*, 7061.
- (7) Chen, G. J.-J.; McDonald, J. W.; Newton, W. E. *Inorg. Chim. Acta* **1980**, *41*, 49.
- (8) Wiegardt, K.; Holzbach, W.; Hofer, E.; Weiss, J. *Inorg. Chem.* **1981**, *20*, 343.
- (9) Young, C. G.; Broomhead, J. A.; Boreham, C. J. *J. Chem. Soc., Dalton Trans.* **1983**, 2135.
- (10) (a) Ricard, L.; Weiss, R. *Inorg. Nucl. Chem. Lett.* **1974**, *10*, 217. (b) Dirand, J.; Ricard, L.; Weiss, R. *Inorg. Nucl. Chem. Lett.* **1975**, *11*, 661.
- (11) (a) Newton, W. E.; McDonald, J. W.; Corbin, J. L.; Ricard, L.; Weiss, R. *Inorg. Chem.* **1980**, *19*, 1997. (b) Marabella, C. P.; Enemark, J. H.; Newton, W. E.; McDonald, J. W. *Inorg. Chem.* **1982**, *12*, 623.

- (12) (a) Isbell, A. F., Jr.; Sawyer, D. T. *Inorg. Chem.* **1971**, *10*, 2449. (b) DeHayes, L. J.; Faulkner, H. C.; Doub, W. H., Jr.; Sawyer, D. T. *Inorg. Chem.* **1975**, *14*, 2110. (c) Hyde, J.; Venkatasubramanian, K.; Zubietta, J. *Inorg. Chem.* **1978**, *17*, 414. (d) Spence, J. T. In *Molybdenum and Molybdenum-Containing Enzymes*; Coughlan, M. P., Ed.; Pergamon: Oxford, 1980; Chapter 3. (e) Cliff, C. A.; Fallon, G. D.; Gatehouse, B. M.; Murray, K. S.; Newman, P. J. *Inorg. Chem.* **1980**, *19*, 773. (f) Charney, L. M.; Schultz, F. A. *Inorg. Chem.* **1980**, *19*, 1527. (g) Rajan, O. A.; Chakravorty, A. *Inorg. Chem.* **1981**, *20*, 660. (h) Topich, J. *Inorg. Chem.* **1981**, *20*, 3704. (i) Lamache, M.; Sanbuichi, F. *Electrochim. Acta* **1981**, *26*, 1525. (j) Charney, L. M.; Finklea, H. O.; Schultz, F. A. *Inorg. Chem.* **1982**, *21*, 549. (k) Pickett, C.; Kumar, S.; Vella, P. A.; Zubietta, J. *Inorg. Chem.* **1982**, *21*, 908. (l) Ghosh, P.; Chakravorty, A. *Inorg. Chem.* **1983**, *22*, 1322. (m) Rajan, O. A.; Spence, J. T.; Leman, C.; Minelli, M.; Sato, M.; Enemark, J. H.; Kroneck, P. M. H.; Sulger, K. *Inorg. Chem.* **1983**, *22*, 3065. (n) Chaudhury, M. J. *Chem. Soc., Dalton Trans.* **1984**, 115. (o) Ledon, H.; Varescon, F.; Malinski, T.; Kadish, K. M. *Inorg. Chem.* **1984**, *23*, 261. (p) Subramanian, P.; Spence, J. T.; Ortega, R.; Enemark, J. H. *Inorg. Chem.* **1984**, *23*, 2564. (q) Bristow, S.; Garner, C. D.; Pickett, C. J. *J. Chem. Soc., Dalton Trans.* **1984**, 1617. (r) Corbin, J. L.; Miller, K. F.; Pariyadath, N.; Wherland, S.; Bruce, A. E.; Stiefel, E. I. *Inorg. Chim. Acta* **1984**, *90*, 41. (s) Backes-Dahmann, G.; Hermann, W.; Wiegardt, K.; Weiss, J. *Inorg. Chem.* **1985**, *24*, 485. (t) Berg, J. M.; Holm, R. H. *J. Am. Chem. Soc.* **1985**, *107*, 917. (u) Kaul, B. B.; Enemark, J. H.; Merbs, S. L.; Spence, J. T. *J. Am. Chem. Soc.* **1985**, *107*, 2885.